Current Optics and Photonics
Vol. 5, No. 1, February 2021, pp. 72–76

ISSN: 2508-7266(Print) / ISSN: 2508-7274(Online)
DOI: https://doi.org/10.3807/COPP.2021.5.1.072

Polarization Ellipticity of Micro-photoluminescence in a Single GaAs/AlGaAs Quantum Ring

Minju Kim[1†], Juyeong Jang[1†], Seunghwan Lee[1†], Jindong Song[2], and Kwangseuk Kyhm[1]*

[1]Department of Opto-mechatronics and Cogno-mechatronics Engineering, Pusan National University, Busan 46241, Korea
[2]Nano-Photonics Research Center, KIST, Seoul 02792, Korea

(Received November 5, 2020 : revised December 16, 2020 : accepted December 24, 2020)

The polarized micro-photoluminescence spectrum was analyzed to investigate the anisotropic localized states in a single GaAs quantum ring. An energy difference of ~0.1 meV was observed from the perpendicularly polarized spectrum measured by a pair of linear analyzers. Spectral dependence of the polarized emission was also characterized in terms of rotation and ellipticity angles using four Stokes parameters. While the rotation angle indicates the symmetric axis of an anisotropic quantum ring with a small variation (± 2°), the ellipticity angle varies from 7.4° down to –2.5°. We conclude that optical anisotropy and birefringence are induced by the crescent-like lateral shape of localized states.

Keywords : Quantum ring, Stokes parameter, Photoluminescence, Spectrum analysis
OCIS codes : (160.4236) Nanomaterials; (250.5230) Photoluminescence; (260.5430) Polarization

I. INTRODUCTION

Lately, the droplet epitaxy technique enables growth of quantum rings (QRs) on a nanometer scale (~50 nm) [1–3]. Regarding the closed path of a rim, QRs were considered as a platform to observe the Aharaonov-Bohm (AB) effect. In mesoscopic ring systems (~1 μm), extremely low temperature (< 100 mK) is necessary to measure the AB effect due to the fragile quantum coherence. However, the small size of QRs (~50 nm) is beneficial for measuring the ABs effect up to tens of Kelvin [4–8].

Although the lateral image of QRs recalls an ideal ring, the height of QRs was known to be anisotropic. Due to the rim anisotropy of a volcano shape, the wavefunction is known to be localized with a crescent shape [9–11]. Regarding quantum dots (QDs) grown by the Stranski-Krastanov method, the elliptical lateral shape is characterized with two perpendicular symmetric axes. However, the crescent-like localized state in a QR has a single symmetric axis. In this case, a different polarization dependence is expected compared to that of elliptical QDs.

Recently, the rim anisotropy of a single quantum ring was studied in terms of linear polarization dependence of micro-photoluminescence (micro-PL) [11, 12], and the rim anisotropy was shown to give rise to localized states with a crescent shape. In this case, the polarization anisotropy is very different from that of elliptical QDs grown by the Stranski-Krastanov (SK) method, and the two eigenstates of elliptical QDs can be accessed through a pair of perpendicular analyzers. However, linear polarization analysis is not enough to characterize the polarization states of the crescent-like localized states. In this work, we have analyzed the polarized micro-PL spectrum from a single quantum ring using four Stokes parameters, where the polarization states of the crescent-like localized states were characterized in terms of ellipticity and rotation angles.

II. METHODS

QRs were grown on GaAs (001) substrate by the droplet epitaxy method, then capped with 53 nm-thick AlGaAs barrier by migration enhanced epitaxy. The sample under-

[†]These authors contributed equally to this paper.
*Corresponding author: kskyhm@pusan.ac.kr, ORCID 0000-0003-3646-3560
Color versions of one or more of the figures in this paper are available online.

went an annealing step in the chamber and was subjected to the rapid thermal annealing process at 800 °C to enhance optical measurements. 404 nm-diode pulsed laser operating at 80 MHz repetition rate was used for excitation. For polarization analysis, a pair of linear polarizers and quarter-waveplates were used. Sample was cooled down to 5 K in a helium flow cryostat, and time-integrated PL spectrum was measured by a charge-coupled device (CCD) camera. A long-pass filter (> 500 nm) was used in order to remove the second order laser peak (808 nm).

III. RESULTS AND DISCUSSION

In Fig. 1(a), uncapped ring structures were seen by a field emission scanning electron microscope (FESEM), whereby we found the density of QRs (~4 × 10^9 cm^{-2}) is low enough to perform micro-PL. As shown schematically in Fig. 1(b), it was known that the anisotropy of rim height results in a pair of localized states with a crescent shape [6, 8, 12]. When the rim height anisotropy of QRs is considered, the adiabatic potential energy $\varepsilon(r,\phi)$ can be obtained theoretically, where r and ϕ are radius and azimuthal angle in the polar coordinates, respectively. For example, the adiabatic potential energy $\varepsilon(r,\phi = 0°)$ at $\phi = 0°$ has a deep energy valley compared to that at ϕ~30°. When the linearly polarized emission along a selected azimuthal angle ϕ appears at different spectrum energy. Therefore, the anisotropic energy structure of $\varepsilon(r,\phi)$ gives rise to a broad PL spectrum, where the confinement levels show different polarization over the large linewidth (~0.4 meV) .

In Fig. 1(c), polarization dependence of micro-PL spectrum was measured from a single QR for changing linear analyzer angle (θ). While θ is decreased from 90° to 0°, the polarized PL intensity becomes decreased with a blueshift. The linearly polarized PL along $\theta = 0°$ originates from the exciton dipoles confined parallel to the symmetric axis of a QR ($\phi = 0°$). Comparing the two peak energy of the perpendicularly polarized PL spectrum measured at θ = 0° (1.6258 eV) and θ = 90° (1.6259 eV), an energy difference (Δ~0.1 meV) was obtained. It is noticeable that micro-PL at a selected wavelength shows both horizontal ($\theta = 0°$) and vertical ($\theta = 90°$) polarizations, whilst the linewidth at 0° (~0.25 meV) is less than that at 90° (~0.35 meV).

In the case of elliptical quantum dots grown by the Stranski-Krastanov(SK) method, the exciton ground states were known to show two separate PL spectra, where their polarizations are perpendicular to each other, and the two eigenstates are determined by not only the anisotropic electron-hole exchange interaction but also the geometric asymmetry of elliptical QDs. Therefore, one of the polarized doublet spectrum can be selected with a linear polarizer parallel to the symmetric axis of an elliptical QD. However, the symmetry of QRs is reduced further when the crescent shape of the localized states is considered. In this case, linear polarization analysis is limited to characterize the localized states of QRs.

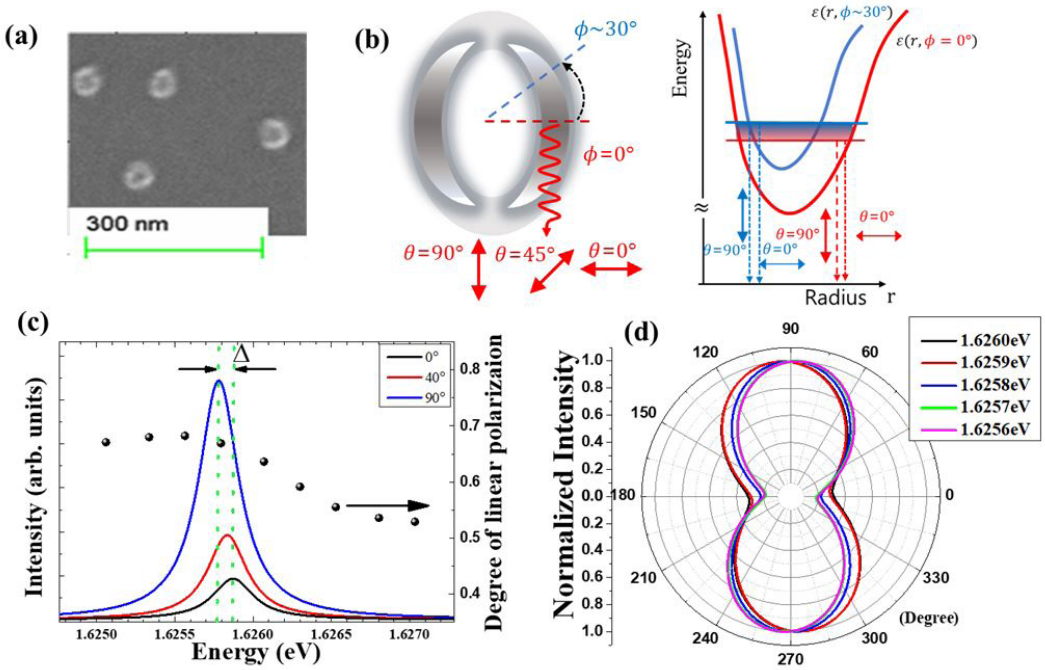

FIG. 1. Polarization dependence of a single quantum ring. (a) FESEM image of uncapped GaAs quantum rings. (b) Due to the anisotropy of the adiabatic potential of a single quantum, the confinement states are likely localized with a crescent-like shape. (c) Micro-PL spectra were observed for three analyzer angles ($\theta = 0°$, 45°, 90°), where an energy difference (Δ~0.1 meV) was observed between the perpendicular polarizations ($\theta = 0°$ and 90°) , the degree of linear polarization was plotted for spectrum energy, and (d) Polarization dependence of normalized PL intensity at different PL energy was plotted for analyzer angle (θ).

As shown in Fig. 1(c), a distinct doublet is not seen in the PL spectrum for changing analyzer angle. When PL intensity at a certain spectrum energy is plotted for analyzer angle, a peanut shape is obtained in Fig. 1(d). However, the PL intensity is not suppressed completely when the analyzer angle is rotated from $\theta = 90°$ to $\theta = 0°$. The angle dependent PL intensity can be evaluated in terms of degree of linear polarization (DLP). In Fig. 1(c), the DLP ranges from 0.55 and up to 0.67. The spectral dependence of the DLP suggests a shape variation of the localized states for a subtle change of confinement energy, i.e. the ellipticity of the crescent shape localized states is enhanced as confinement is enhanced. As a result, the DLP becomes also enhanced for increased spectrum energy. Additionally, a large spectral difference (Δ~0.1 meV) was obtained with a perpendicular analyzer pair. Compared with that of elliptical SK-QDs (~tens of μeV), this value is larger by an order of magnitude. Therefore, the reduced symmetry of the crescent shape localized states possibly gives rise to an elliptical polarization with a phase retardation.

When a phase retardation is also involved, the polarization state should be considered elliptical. In this case, a pair of linear analyzers are not enough to characterize the phase retardation of an elliptical polarization, and wave-plates are also necessary. In general, an arbitrary elliptical polarization state can be characterized by four Stokes parameters [13]. Suppose electric fields of E_x and E_y are defined along the horizontal ($\theta = 0°$) and vertical ($\theta = 90°$) axes, the four Stokes parameters are determined as

$$S_0 = E_x E_x^* + E_y E_y^*, \quad (1)$$

$$S_1 = E_x E_x^* - E_y E_y^*, \quad (2)$$

$$S_2 = E_x E_y^* + E_y E_x^*, \quad (3)$$

$$S_3 = i(E_x E_y^* - E_y E_x^*), \quad (4)$$

where both E_x and E_y are complex numbers. In order to obtain the Stokes parameters through optical measurements, a linear polarizer and a wave-plate are positioned before the detector. First, the polarized PL is transmitted through a wave-plate to induce a phase retardation angle (φ), then detected by a linear polarizer with an analyzer angle (θ). As a result, the detected intensity $I(\theta,\varphi)$ can be obtained from the four Stokes parameters as

$$I(\theta,\varphi) = \frac{1}{2}[S_0 + S_1 \cos 2\theta + S_2 \cos\varphi \sin 2\theta + S_3 \sin\varphi \sin 2\theta], \quad (5)$$

which is the so-called Stokes' intensity formula.

In Fig. 2(a), micro-PL spectrum were measured at four different polarization configurations of $I(\theta,\varphi)$. While either $\varphi = 90°$ or $\varphi = 0°$ was selected for phase retardation angle, three angles ($\theta = 0°$, 45°, 90°) were used for analyzer angle. As a result, four spectra of the Stokes parameters were obtained from the four different spectra of $I(\theta,\varphi)$,

$$S_0 = \frac{1}{p^2}[I(0°,0°) + I(90°,0°)], \quad (6)$$

$$S_1 = \frac{1}{p^2}[I(0°,0°) - I(90°,0°)], \quad (7)$$

$$S_2 = \frac{1}{p^2}[2I(45°,0°) - I(0°,0°) - I(90°,0°)], \quad (8)$$

$$S_3 = \frac{1}{p^2}[2I(45°,90°) - I(0°,0°) - I(90°,0°)], \quad (9)$$

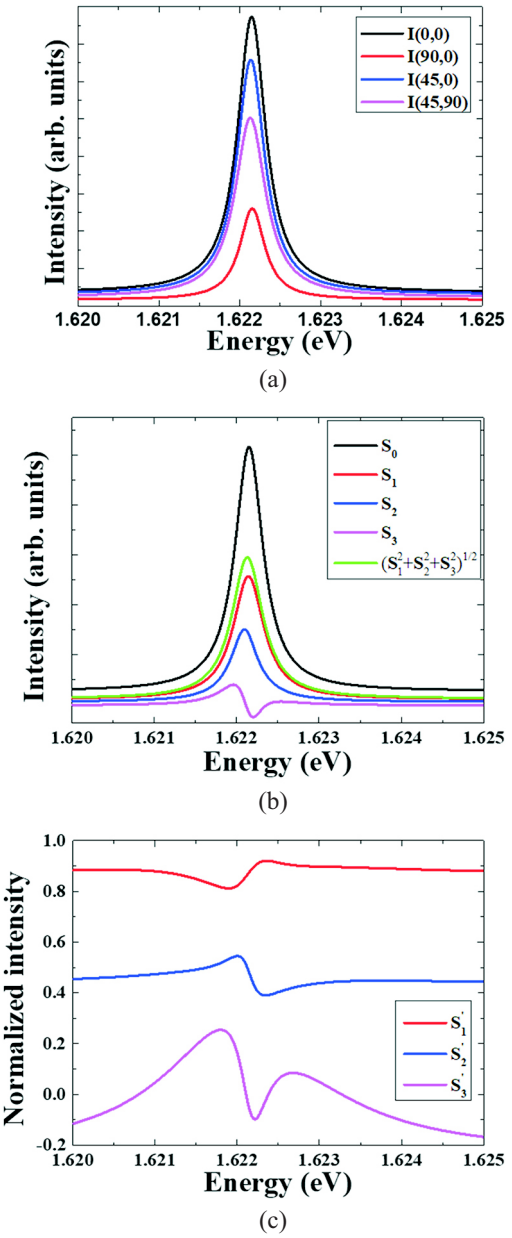

FIG. 2. Stokes parameter spectrum. (a) Micro-PL spectra were obtained for changing linear analyzer angle (θ) and phase retardation angle (ϕ), whereby the four spectra of Stokes parameters (S_0, S_1, S_2, and S_3) were also obtained (b), and (c) Coherent spectrum was analyzed in terms of normalized spectra of S_1, S_2, and S_3.

where p^2 is the absorption factor of analyzers. Although the absorption factor affects the magnitude of detected intensity, but contributes as a denominator in the four Stokes parameters. However, it is cancelled out when the ratio of two Stokes parameters is considered.

Figure 2(b) shows the spectrum of four Stokes parameters (S_0, S_1, S_2, and S_3), where the first Stokes parameter S_0 is the total intensity of light, and the positive/negative magnitude of S_1, S_2, and S_3 represent a degree of horizontal/vertical linear polarization, diagonal/anti-diagonal linear polarization, and left/right circular polarization, respectively. It is noticeable that the polarized intensity $S = (S_1^2 + S_2^2 + S_3^2)^{1/2}$ is less than S_0, which is the radius of the Poincaré sphere. In order to evaluate the emission coherence, a degree of coherence polarization (P) can be obtained by

$$P = \frac{\int (S_1^2+S_2^2+S_3^2)^{1/2} d\omega}{\int S_0 d\omega}. \quad (10)$$

We obtained $P \sim 0.6$, which implies 40% of the PL spectrum is incoherent. Recently, we have also observed ~25 ps of coherence time from a single QR [14]. This value is short by an order of magnitude compared to that of SK QDs, and suggests the presence of decoherent scatterings between the various confinement levels of the localized states. It is noticeable that the degree of coherence polarization (P) is not equivalent to the degree of linear polarization (DLP). While DLP shows an asymmetry of the localized states in terms of linear polarization, P provides the portion of coherence emission to observed in PL.

In Fig. 2(c), the three Stokes parameters of S_1, S_2, and S_3 were normalized by S, i.e. $S_1' = S_1/S$, $S_2' = S_2/S$, $S_3' = S_3/S$. It is clear that the polarization state of coherent PL consists of not only linear polarizations but also phase retardations. As a result, the linearly polarized components are aligned with an angle between $\theta = 0°$ and $\theta = 45°$, but elliptical polarization components are also present with a phase retardation $\varphi < 90°$.

As inset shows schematically in Fig. 3(a), an arbitrary polarization state can be specified in terms of rotation angle (ψ) and ellipticity angle (χ). With two perpendicular axes of x and y, the rotation angle (ψ) of an elliptical polarization is given by an angle between the x-axis and the major axis of an ellipse. If a phase retardation is involved, the ellipticity angle (χ) is also determined by the major and minor axes of an ellipse. Given the normalized Stokes parameters (S_1', S_2', S_3'), where S_1, S_2, and S_3 were divided by $(S_1^2 + S_2^2 + S_3^2)^{1/2}$, we obtained ψ and χ by

$$\psi = \frac{1}{2}\tan^{-1}\left(\frac{S_2'}{S_1'}\right), \quad (11)$$

$$\chi = \frac{1}{2}\sin^{-1}(S_3'). \quad (12)$$

In Fig. 3(a), the spectrum of ψ and χ were compared with polarization independent PL intensity, which was measured without any analyzer. In Fig. 3(b), various elliptical polarizations near the dominant PL spectrum were also plotted in term of the Jones vector components (E_x, E_y), and each polarization state was also mapped in Poincaré space as shown in Fig. 3(c). Interestingly, ψ was observed to be nearly constant (~13°) at both the spectral wing sides, but a relatively drastic change was seen near the dominant PL spectrum. Provided that the electron-hole pair confined

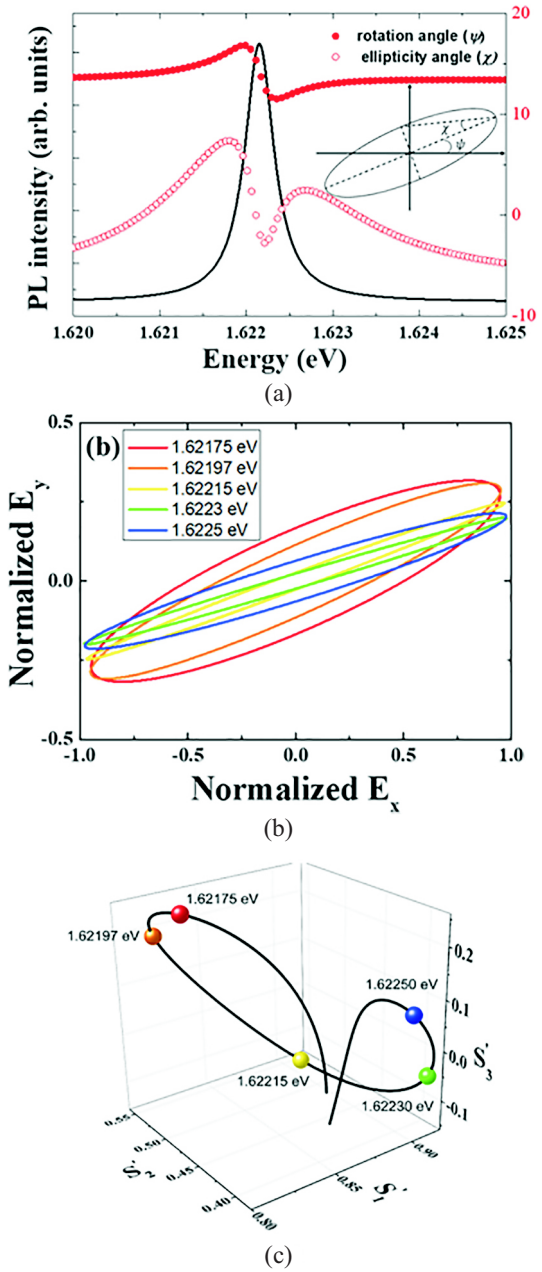

FIG. 3. Polarization ellipticity of a single quantum ring. (a) Spectrum of rotation (ψ) and ellipticity (χ) angles, whereby elliptical polarization can be specified. (b) Various elliptical polarizations at different energy were shown with two perpendicular normalized electric fields (E_x and E_y), and (c) Normalized Stokes parameters at different spectrum energy were plotted in a Poincaré sphere.

along a certain orientation in the crescent-like structure gives rise to a linear polarization along the dipole oscillation direction at a specific spectrum energy, the constant rotation angle (ψ~13°) corresponds to the symmetric axis of a QR (θ = 90° and ϕ = 90°). As it depends on the position of sample, rotation in the lateral plane gives a different value.

The large confinement size along the symmetric axis is also expected to have a large oscillator strength. Therefore, the low-energy PL near θ = 90° dominates while the high-energy PL polarized along θ = 0° becomes suppressed. However, the anisotropy of crescent-like localized structures results in a variation of ψ (16.8°–11.5°) near the dominant PL spectrum. Additionally, the asymmetry of the localized structure gives rise to a birefringence. Although a confinement energy level is given by the anisotropic potential structure of $\varepsilon(r,\phi)$ in Fig. 1(b), the exciton wavelengths in the crescent-like localized structure change the orientation ϕ. Consequently, the anisotropy of $\varepsilon(r,\phi)$ leads to an optical phase retardation. As shown in Fig. 3(a), χ varies from –2.5° up to 7.3° near the dominant PL spectrum. When PL spectrum is determined from the confinement levels of $\varepsilon(r,\phi)$, the optical asymmetry still remains within the linewidth. Therefore, a spectrum of χ represents the asymmetry of the lateral wavefunction.

IV. CONCLUSION

We have analyzed the polarization of the micro-PL spectrum from a single quantum ring, where rotation and ellipticity angles were obtained for spectrum energy. Those results have confirmed the presence of anisotropic localized states, and we conclude that the crescent-like lateral shape induces a birefringence, resulting in various elliptical polarization states for spectrum energy.

ACKNOWLEDGMENT

This study was supported by a grant from The Competency Development Program for Industry Specialist (P0008763) and National Research Foundation (NRF-2020R1A2C1005973).

REFERENCES

1. T. Mano, T. Kuroda, K. Kuroda, and K. Sakoda, "Self-assembly of quantum dots and rings by droplet epitaxy and their optical properties," J. Nanophoton. **3**, 031605 (2009).
2. C. Somaschini, S. Bietti, S. Sanguinetti, N. Koguchi, and A. Fedorv, "Self-assembled GaAs/AlGaAs coupled quantum ring-disk strucures by droplet epitaxy," Nanotechnology **21**, 125601 (2010).
3. T. Kuroda, T. Mano, T. Ochiai, S. Sanguinetti, K. Sakoda, G. Kido, and N. Koguchi, "Optical transitions in quantum ring complexes," Phys. Rev. B **72**, 205301 (2005).
4. A. Lorke, R. J. Luyken, A. O. Govorov, J. P. Kotthaus, J. M. Garcia, and P. M. Petroff, "Spectroscopy of nanoscopic semiconductor rings," Phys. Rev. Lett. **84**, 2223 (2000).
5. A. O. Govorov, S. E. Ulloa, K. Karrai, and R. J. Warburton, "Polarized excitons in nanorings and the optical Aharonov-Bohm effect," Phys. Rev. B **66**, 081309 (2002).
6. H. D. Kim, R. Okuyama, K. Kyhm, M. Eto, R. A. Taylor, A. L. Nicolet, M. Potemski, G. Nogues, L. S. Dang, K. -C. Je, J. Kim, J. -H. Kyhm, K. H. Yoen, E. H. Lee, J. Y. Kim, I. K. Han, W. Choi, and J. Song, "Observation of a biexciton Wigner molecule by fractional optical Aharonov-Bohm oscillations in a single quantum ring," Nano Lett. **16**, 27–33 (2016).
7. Z. Barticevic, G. Fuster, and M. Pacheco, "Effect of an electric field on the Bohm-Aharonov oscillations in the electronic spectrum of a quantum ring," Phys. Rev. B. **65**, 193307 (2002).
8. N. A. J. M. Kleemans, I. M. A. Bominaar-Silkens, V. M. Fomin, V. N. Gladilin, D. Granados, A. G. Taboada, J. M. García, P. Offermans, U. Zeitler, P. C. M. Christianen, J. C. Maan, J. T. Devreese, and P. M. Koenraad, "Oscillatory persistent currents in self-assembled quantum rings," Phys. Rev. Lett. **99**, 146808 (2007).
9. V. M. Fomin, *Physics of Quantum Rings*, 2nd ed., (Springer, Berlin, Germany, 2018).
10. S. Park, J. Kim, J. Takayama, A. Murayama, and K. Kyhm, "Carrier relaxation dynamics between localized vertical confinement states in GaAs/AlGaAs quantum rings," J. Korea Phys. Soc. **73**, 314–319 (2018).
11. H. D. Kim, K. Kyhm, R. A. Taylor, A. A. L. Nicolet, M. Potemski, G. Nogues, K. C. Je, E. H. Lee, and J. D. Song, "Excited exciton biexciton localised states in a single quantum ring," Appl. Phys. Lett. **103**, 173106 (2013).
12. H. D. Kim, K. Kyhm, R. A. Taylor, G. Nogues, K. C. Je, E. H. Lee, and J. D. Song, "Asymmetry of localised states in a single quantum ring: Polarization dependence of excitons and biexcitons," Appl. Phys. Lett. **102**, 033112 (2013).
13. D. H. Goldstein, *Polarized Light*, 3rd ed., (CRC Press, BR, USA, 2011).
14. M. Kim, S. Park, Y. Yamashita, K. Kyhm, M. Ikezawa, S. Bietti, and S. Sanguinetti, "Decoherence dynamics of localized states in a single GaAs/AlGaAs quantum ring," Phys. Status Solidi **12**, 1800176 (2018).